Hot Corrosion Behaviour of 18Cr–8Ni Austenitic Steel in Presence of Na$_2$SO$_4$ and Transition Metal Salts

By A. U. Malik*, M. Misbahul Amin* and Sharif Ahmad*

The high temperature oxidation behaviour of 18Cr–8Ni austenitic steel has been studied in presence of Na$_2$SO$_4$ and transition metal salts, e.g. NiSO$_4$, CoSO$_4$, Cr$_2$(SO$_4$)$_3$, (NH$_4$)$_2$MoO$_4$, NaVO$_3$ or Na$_2$WO$_4$ in the temperature range of 923–1273 K in air.

The steels coated with a mixture of Na$_2$SO$_4$+NiSO$_4$ and Na$_2$SO$_4$+CoSO$_4$ show higher corrosion rates than either the Na$_2$SO$_4$ coated or transition metal sulphate coated steel at 923 K. This has been attributed to the formation of low temperature eutectics. At 1273 K, except the Cr$_2$(SO$_4$)$_3$ or CoSO$_4$ coated steel, the steel coated with all other salts, e.g. Na$_2$WO$_4$, NaVO$_3$ or (NH$_4$)$_2$MoO$_4$, have much higher corrosion rates than the Na$_2$SO$_4$ coated steel. The decomposition of these salts into volatile oxides, e.g. WO$_3$, V$_2$O$_5$ or MoO$_3$ seems to be the sole reason for catastrophic oxidation. A direct oxidation or sulphidation cum fluxing mechanism is adequate to explain hot corrosion. The scale morphology as predicted from mechanistic considerations is in fairly good agreement with the observed morphology.

I. Introduction

Iron-base alloys containing chromium as a major constituent with nickel additions are the most prominent materials in coal-fired power generating units and petroleum refinery plants. The corrosion of these alloys under servicing conditions is not uncommon due to the deposition of the molten salt(s) or ash and/or the attack of gaseous species such as O$_2$, CO, CO$_2$, SO$_2$, H$_2$S etc. A fairly large number of investigations have been carried out on steels dealing with fire-side deposit corrosion[1]–[3]. Alkali sulphates are the most frequent deposits on alloy component surfaces and are responsible for hot corrosion attack at relatively low temperatures due to formation of low melting eutectics[4]–[6], e.g. Na$_2$SO$_4$+Fe$_2$(SO$_4$)$_3$ (873 K), K$_2$SO$_4$+Fe$_2$(SO$_4$)$_3$ (900 K), K$_2$SO$_4$+Na$_2$SO$_4$+Fe$_2$(SO$_4$)$_3$ (813 K), etc. However, besides Fe$_2$(SO$_4$)$_3$, the role of salts of other transition metals (present as alloy additions) has not been studied either alone or in presence of Na$_2$SO$_4$, although such studies have been

done on nickel and cobalt-base alloys. Recently low temperature hot corrosion studies have been reported by Luthra and Jones *et al.*[8][9] on nickel and cobalt base alloys, in which formation of low melting eutectics, e.g. NiSO$_4$+Na$_2$SO$_4$ (940 K) and CoSO$_4$+Na$_2$SO$_4$ (928 K), respectively, seems to be an important factor responsible for inducing hot corrosion at temperatures as low as 873 K.

The present investigation was undertaken to examine the effect of some transition metal salts or their mixtures with Na$_2$SO$_4$ on the oxidation behaviour of a commercial 18Cr–8Ni austenitic steel in the temperature range of 923–1273 K.

II. Experimental

Coupons of 18 mm × 12 mm × 1 mm size were cut from a sheet of a commercial austenitic steel (Cr: 18%, Ni: 8%, Mn: 4%, C: 0.15%, Fe: balance) and were homogenized at 1173 K for 144 ks in an evacuated quartz tube (pressure: 1.35×10^{-2} Pa). The specimens were abraded sequentially with 180, 320 and 600 grade SiC papers.

The polished specimens were uniformly coated with relatively thin films of Na$_2$SO$_4$, transition metal salts: Cr$_2$(SO$_4$)$_3$, NiSO$_4$, CoSO$_4$, NaVO$_3$, Na$_2$WO$_4$ or (NH$_4$)$_2$MoO$_4$ or

* Chemistry Section, Z. H. College of Engineering and Technology, Aligarh Muslim University, Aligarh (U.P.), India.

Table 1   Constituents in scales of the oxidation alloys as identified by X-ray diffraction analysis.

Coating on steel	Temp. K	Constituents identified	Coating on steel	Temp. K	Constituents identified
Na$_2$SO$_4$	923	Cr$_2$O$_3$, FeO, Fe$_2$O$_3$	Na$_2$WO$_4$	1123	Cr$_2$O$_3$, FeO·WO$_3$, WO$_3$, Fe$_2$O$_3$, Na$_2$O·FeO$_2$
Na$_2$SO$_4$	1123	Cr$_2$O$_3$, Cr$_2$S$_3$, FeO, Fe$_2$O$_3$			
Na$_2$SO$_4$	1273	FeS, Cr$_2$S$_3$, FeO, Fe$_2$O$_3$, Na$_2$FeO$_2$	Na$_2$WO$_4$	1273	Cr$_2$O$_3$, FeO·WO$_3$, Na$_2$FeO$_2$
Na$_2$SO$_4$+Cr$_2$(SO$_4$)$_3$	923	Cr$_2$O$_3$, FeO, Na$_2$FeO$_2$	Na$_2$SO$_4$+Na$_2$WO$_4$	923	FeO·WO$_3$, Na$_2$FeO$_2$, WO$_3$, Cr$_2$O$_3$, Fe$_2$O$_3$
Na$_2$SO$_4$+Cr$_2$(SO$_4$)$_3$	1123	Cr$_2$O$_3$, FeO, Na$_2$FeO$_2$	Na$_2$SO$_4$+Na$_2$WO$_4$	1123	FeO·WO$_3$, Na$_2$FeO$_2$, WO$_3$, Cr$_2$O$_3$, Fe$_2$O$_3$
Na$_2$SO$_4$+Cr$_2$(SO$_4$)$_3$	1273	Cr$_2$S$_3$, Cr$_2$O$_3$, FeO, Na$_2$FeO$_2$	Na$_2$SO$_4$+Na$_2$WO$_4$	1273	FeCr$_2$S$_4$, Cr$_2$S$_3$, Cr$_2$O$_3$, FeO·WO$_3$, FeS, Fe$_2$O$_3$
Cr$_2$(SO$_4$)$_3$	923	Cr$_2$O$_3$, FeO, Fe$_2$O$_3$	NaVO$_3$	923	Cr$_2$O$_3$, V$_2$O$_5$, Na$_2$FeO$_2$, Na$_2$Fe$_2$O$_5$, FeO
Cr$_2$(SO$_4$)$_3$	1123	Cr$_2$O$_3$, FeO, Fe$_3$O$_4$, Fe$_2$O$_3$			
Cr$_2$(SO$_4$)$_3$	1273	Cr$_2$O$_3$, FeO, Fe$_3$O$_4$, Fe$_2$O$_3$	NaVO$_3$	1123	FeO·V$_2$O$_5$, Cr$_2$O$_3$, V$_2$O$_5$, FeO, Fe$_2$O$_3$, Na$_2$FeO$_2$
NiSO$_4$	923	Cr$_2$O$_3$, FeO, NiO, Fe$_2$O$_3$, FeO·NiO	NaVO$_3$	1273	FeO·V$_2$O$_5$, Cr$_2$O$_3$, Na$_2$FeO$_2$
NiSO$_4$	1123	Cr$_2$O$_3$, FeO, NiO, NiS, Fe$_2$O$_3$	Na$_2$SO$_4$+NaVO$_3$	923	Cr$_2$O$_3$, V$_2$O$_5$, Na$_2$FeO$_2$, FeO, Na$_2$SO$_4$
NiSO$_4$	1273	(Fe, Ni)S, Cr$_2$S$_3$, NiS, FeO, Fe$_2$O$_3$	Na$_2$SO$_4$+NaVO$_3$	1123	Cr$_2$O$_3$, FeO·V$_2$O$_5$, Na$_2$FeO$_2$, V$_2$O$_5$, Cr$_2$S$_3$
Na$_2$SO$_4$+NiSO$_4$	923	NiS, NiO, FeO, Cr$_2$O$_3$, FeO, Na$_2$FeO$_2$	Na$_2$SO$_4$+NaVO$_3$	1273	Cr$_2$O$_3$, FeO·V$_2$O$_5$, Na$_2$FeO$_3$, (Fe, Cr)$_2$S$_3$
Na$_2$SO$_4$+NiSO$_4$	1123	NiS, NiO, FeO, Cr$_2$O$_3$, FeO, Na$_2$FeO$_2$	(NH$_4$)$_2$MoO$_4$	923	MoO$_3$, FeO, Cr$_2$O$_3$, Fe$_2$O$_3$
Na$_2$SO$_4$+NiSO$_4$	1273	NiS, Cr$_2$S$_3$, FeS, (Fe, Ni)S, Fe$_2$O$_3$	(NH$_4$)$_2$MoO$_4$	1123	FeO·MoO$_3$, Cr$_2$O$_3$, Fe$_2$O$_3$, NiO
CoSO$_4$	923	CoO, Cr$_2$O$_3$, FeO, Fe$_2$O$_3$	(NH$_4$)$_2$MoO$_4$	1273	FeO·MoO$_3$, FeO, Fe$_2$O$_3$, Cr$_2$O$_3$, NiO
CoSO$_4$	1123	CoO, Cr$_2$O$_3$, FeO, Fe$_3$O$_4$, Fe$_2$O$_3$	Na$_2$SO$_4$+(NH$_4$)$_2$MoO$_4$	923	MoO$_3$, FeO, Cr$_2$O$_3$, Fe$_2$O$_3$, Na$_2$SO$_4$
CoSO$_4$	1273	CoO, Cr$_2$O$_3$, FeO, Fe$_3$O$_4$, Fe$_2$O$_3$, CoSO$_4$	Na$_2$SO$_4$+(NH$_4$)$_2$MoO$_4$	1123	MoO$_3$, FeO, Cr$_2$O$_3$, Fe$_2$O$_3$, Na$_2$SO$_4$
Na$_2$SO$_4$+CoSO$_4$	923	CoO, Cr$_2$O$_3$, FeO, Fe$_2$O$_3$, CoSO$_4$, CoS, FeS	Na$_2$SO$_4$+(NH$_4$)$_2$MoO$_4$	1273	Na$_2$O·MoO$_3$, FeO·MoO$_3$, Fe$_2$O$_3$, Cr$_2$O$_3$, Cr$_2$S$_3$, FeS
Na$_2$SO$_4$+CoSO$_4$	1123	CoO, Cr$_2$O$_3$, FeO, Fe$_2$O$_3$, CoSO$_4$			
Na$_2$SO$_4$+CoSO$_4$	1273	CoSO$_4$, CoO, Cr$_2$O$_3$, Cr$_2$S$_3$, FeS, NiO, FeO	Coating on steel	Temp.	Constituents identified
Na$_2$WO$_4$	923	Cr$_2$O$_3$, FeO·WO$_3$, Na$_2$FeO$_2$, Fe$_2$O$_3$, WO$_3$			

their mixtures. The specimens were heated to about 573 K and were sprayed with aqueous solution of the salt till a nearly uniform coating was obtained. The salt coated specimens were transferred to silica boats and dried in a hot air oven at 383 K for about 6 hours, cooled to room temperature and weighed The oxidation experiments were carried out in a horizontal

tubular furnace in flowing air at three different temperatures, viz. 923, 1123 and 1273 K. The oxidation runs were normally of 36 ks duration.

The different constituents present in the scales of oxidized specimens were identified by X-ray diffraction analysis and are listed in Table 1.

The metallographic studies were carried out using a photometallurgical microscope. The mounted specimens were abraded and polished by conventional means using SiC papers and diamond pastes of various grades, respectively.

The SEM and EDAX studies were carried out using a Cambridge Scanning Electron Microscope S4-10.

III. Results

1. Oxidation studies

Figures 1 to 3 represent some typical curves

showing the effect of salt concentration on the oxidation rates of 18Cr–8Ni steel at different temperatures.

(1) Na_2SO_4

At 1123 and 1273 K, the oxidation rates of Na_2SO_4 coated alloy specimens increase with increasing salt concentration upto a salt deposition of about 20 g m^{-2}. A further increase in the amount of salt deposition results in a decrease in oxidation rates, and the decrease is steep at 1123 K. However, the coated alloy shows a linear increase in oxidation rate with increasing salt deposition at 923 K.

(2) $NiSO_4$ and $CoSO_4$

These salts behave similarly as far as their influence on the oxidation rate of 18Cr–8Ni alloys is concerned. At 923 K the oxidation rates of the steel coated with $Na_2SO_4 + CoSO_4$ or
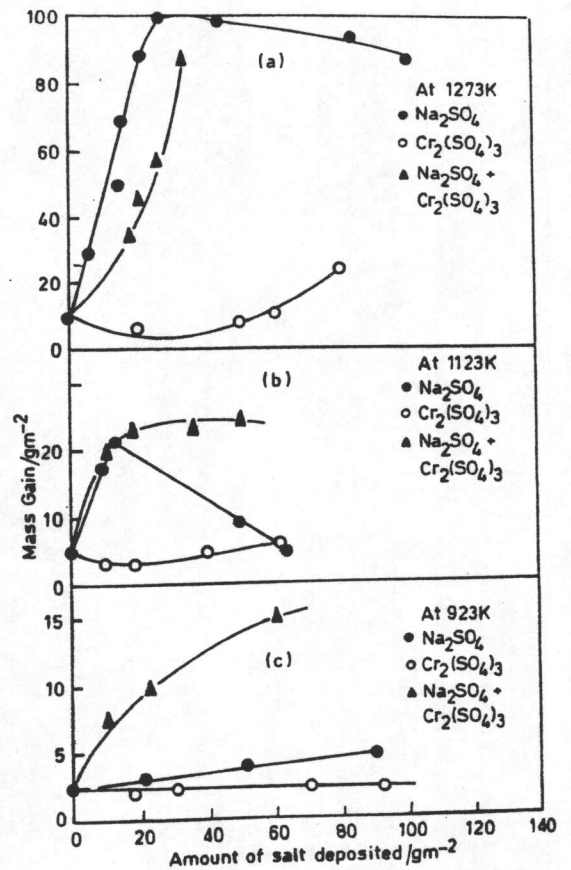

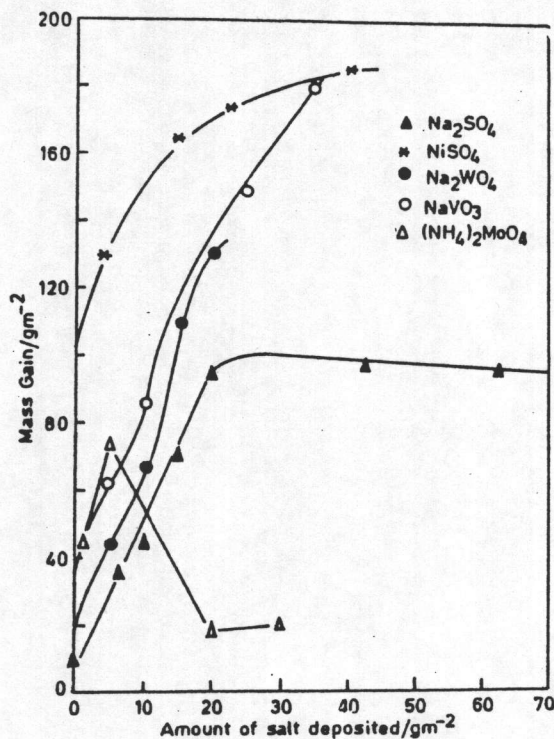Fig. 1 Amount of $CoSO_4$ deposited vs mass gain plots oxidized at 923, 1123 and 1273 K.

Fig. 2 Amount of $Cr_2(SO_4)_3$ deposited vs mass gain plots oxidized at 923, 1123 and 1273 K.

Fig. 3 Amount of Na_2SO_4 and transition metal salts vs mass gain plots oxidized at 1273 K.

$Na_2SO_4 + NiSO_4$ are higher than those coated with $NiSO_4$, $CoSO_4$ or Na_2SO_4. This may be attributed to the formation of low melting eutectic $Na_2SO_4 + NiSO_4$ or $Na_2SO_4 + CoSO_4$ which facilitates corrosion attack. At 1273 K, the role of these salts is reversed and the presence of the salts in Na_2SO_4 lowers the oxidation rate. In fact, Na_2SO_4 coated steel has the highest oxidation rate followed by $CoSO_4$ or $NiSO_4$ coated one (Fig. 1).

(3) $Cr_2(SO_4)_3$

The addition of $Cr_2(SO_4)_3$ to Na_2SO_4 decreases the oxidation rate of the Na_2SO_4 coated alloy at 1123 K and 1273 K. However, an opposite behaviour is observed at 923 K. The oxidation rates of $Cr_2(SO_4)_3$ coated steel are the lowest in the temperature range of 923–1273 K (Fig. 2).

(4) Na_2WO_4, $NaVO_3$ and $(NH_4)_2MoO_4$

The presence of these salts has a deleterious effect on corrosion resistance of 18Cr–8Ni steel. At lower temperature (923 K), this effect is not so marked, especially in tungstate and molybdate coated steels which have lower oxidation rates than Na_2SO_4 coated steel. However, at 1123 K and 1273 K, the steel coated with either of the salts has much higher oxidation rate than the Na_2SO_4 coated steel (Fig. 3).

2.   Morphological studies

Figures 4 and 5 show SEM pictures of Na_2SO_4 coated 18Cr–8Ni steel oxidized at 1123 K and 1273 K, respectively, for 36 ks in flowing air. The grey coloured inner scales are relatively compact and presumably contain sulpho-spinel $FeS \cdot Cr_2S_3$ in predominent concentrations; this is followed by chromium-rich wustite scales, Fe_3O_4/Fe_2O_3 forming the outer scales. The steel specimens coated with varying concentrations of Na_2SO_4 show similar morphological features, though the sulphide phase appears only in the alloy oxidized at 1123 K and 1273 K. The Na_2SO_4-coated steel specimens oxidized at 923 K show the presence of some residual Na_2SO_4 in the form of white deposits. The X-ray concentration profiles indicate the presence of chromium-rich inner layers and iron-rich outer layers. Sulphur is
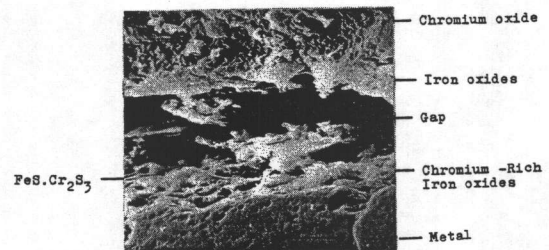

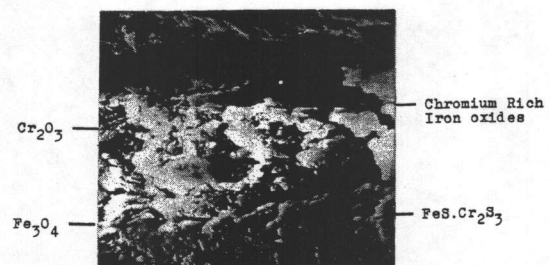Fig. 4   SEM of Na_2SO_4 (3.5 g m⁻²) coated steel oxidized at 1123 K.

Fig. 5   SEM of Na_2SO_4 (19.2 g m⁻²) coated steel oxidized at 1273 K.

present in prediment concentration in the inner layers (Fig. 6).

Some of the coated steel specimens oxidized for more than 36 ks show almost similar surface conditions, although the scales are becoming thicker with increasing exposure time.

Figure 7 shows a SEM picture of the steel coated with $Cr_2(SO_4)_3$ and oxidized at 923 K for 36 ks. The presence of a duplex scale is indicated, the inner scales being rich in chromia (dark grey) followed by porous light grey scales of $FeO \cdot Cr_2O_3$. At higher temperatures similar morphologies are observed, and there is no evidence of sulphide. In $Na_2SO_4 + Cr_2(SO_4)_3$ coated steel, presence of chromium sulphide in the inner layer is indicated at 1123 K and 1273 K. Internal sulphidation occurs due to the penetration of sulphur through the matrix. The X-ray concentration profiles indicate the presence of chromium-rich sulphide layer at the alloy/scale interface, the outer layers being enriched in iron (Fig. 8).

Figures 9 and 10 show SEM pictures of the steel coated with $NiSO_4$ and oxidized at 923 K and 1273 K. The greyish inner scales contain chromia, being followed by outer scales of iron oxide with NiO inclusions; there is an evidence of the presence of NiS particles in the inner scales of the steels oxidized at 1273 K. The steel coated with a mixture of $NiSO_4$ and Na_2SO_4 and oxidized at 923 K shows inner scales of chromia followed by iron oxide scales; there is an evidence of salt penetration through chromia scales and along the grain boundaries in the matrix. The presence of isolated sulphide pockets is also indicated. At 1273 K, there is an evidence of sulphidation which is indicated by the presence of a chromium
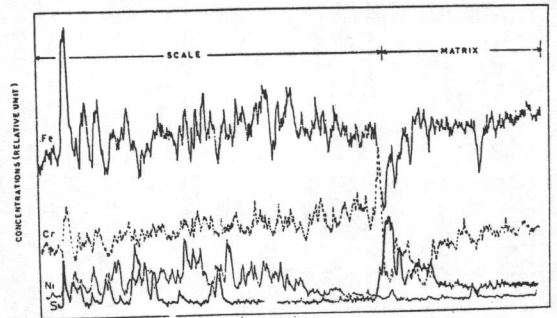

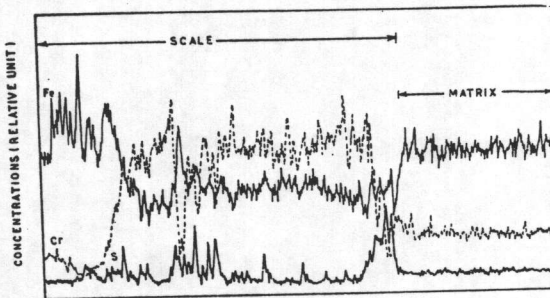Fig. 8   Fe, Cr, Ni and S X-ray profiles across a scale formed on $Cr_2(SO_4)_3$ coated steel oxidized at 1273 K.

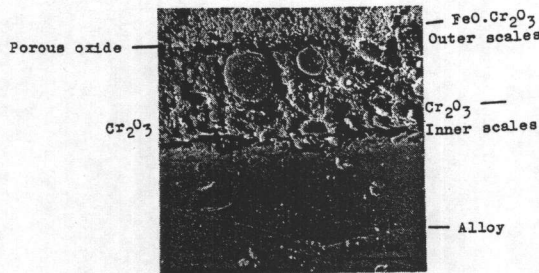Fig. 6   Fe, Cr and S X-ray profiles across a scale formed on Na_2SO_4 coated steel oxidized at 1273 K.

Fig. 9   SEM of $NiSO_4$ (2.4 g m^{-2}) coated steel oxidized at 923 K.

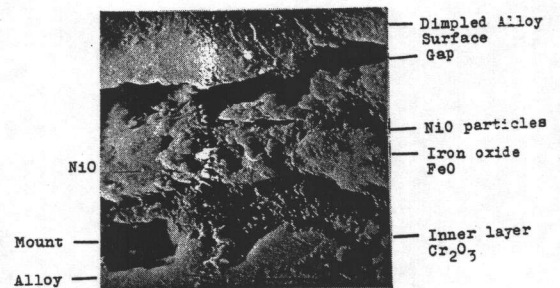Fig. 7   SEM of $Cr_2(SO_4)_3$ (24.0 g m^{-2}) coated steel oxidized at 923 K.
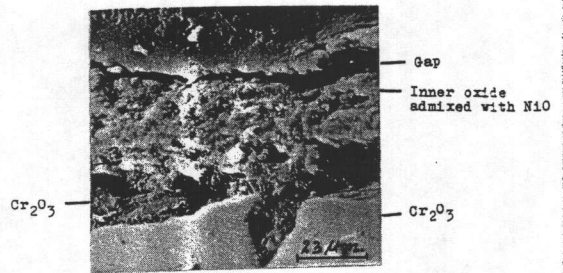

Fig. 10   SEM of $NiSO_4$ (10 g m^{-2}) coated steel oxidized at 1273 K.

sulphide-rich inner layer followed by chromium-iron oxide scales containing NiS inclusions. The X-ray concentration profiles indicate the same elemental distribution in the scales (Fig. 11).

Figure 12 shows a photomicrograph of the alloy coated with Na$_2$WO$_4$ and oxidized at 1273 K. WO$_3$ forms inner layers of the scales followed by chromium-rich iron oxide layers. The SEM picture of the alloy coated with Na$_2$SO$_4$ and Na$_2$WO$_4$ shows the presence of
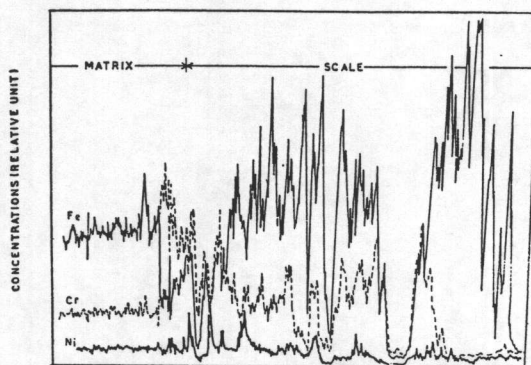
chromium sulphides in the inner layers followed by iron oxide scales rich in WO$_3$ (Fig. 13). The X-ray concentration profiles of the oxidized steel provide similar information (Fig. 14).
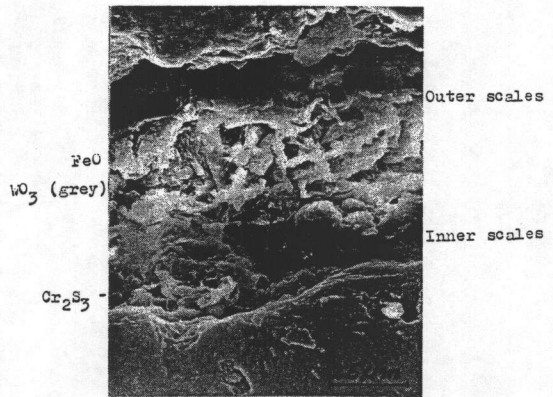

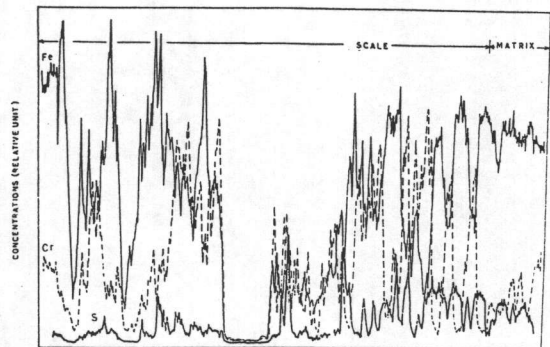Fig. 13   SEM of Na$_2$SO$_4$+Na$_2$WO$_4$ coated steel oxidized at 1273 K.

Fig. 11   Fe, Cr and Ni X-ray profiles across a scale formed on NiSO$_4$ coated steel oxidized at 1273 K.

Fig. 14   Fe, Cr and S X-ray profiles across a scale formed on (Na$_2$SO$_4$+Na$_2$WO$_4$) coated steel oxidized at 1273 K.
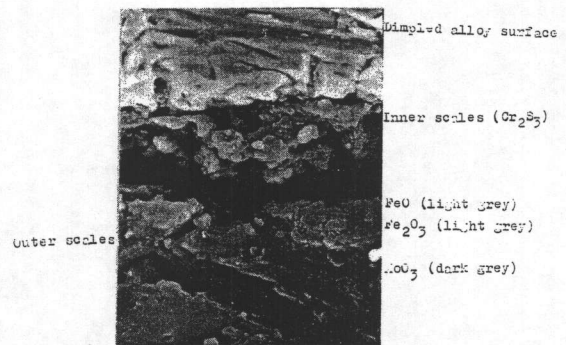

Fig. 12   Microstructure of Na$_2$WO$_4$ coated steel oxidized at 1273 K.

Fig. 15   SEM of Na$_2$SO$_4$+(NH$_4$)$_2$MoO$_4$ (9.8+5.0 g m^{-2}) coated steel oxidized at 1273 K.

Figure 15 shows a SEM picture of the steel coated with Na_2SO_4 and $(NH_4)_2MoO_4$. MoO_3 appeared as an external layer containing inclusions of Fe_2O_3, and the inner scales are rich in chromium sulphide. The X-ray concentration profiles indicate the presence of chromium-rich inner scales (Fig. 16).

The photomicrograph of the alloy coated with $NaVO_3$ and oxidized at 1273 K shows the presence of iron oxide with V_2O_5 inclusions in the outer layers of the scales. There is some evidence of the penetration of the molten salt into the matrix. The SEM picture of the steel coated with Na_2SO_4 and $NaVO_3$ and oxidized at 1273 K shows the presence of dark V_2O_5 in the outer layers of the scales, the middle layers presumably contain $FeO \cdot V_2O_5$ and the inner layers are rich in Cr_2S_3 (Fig. 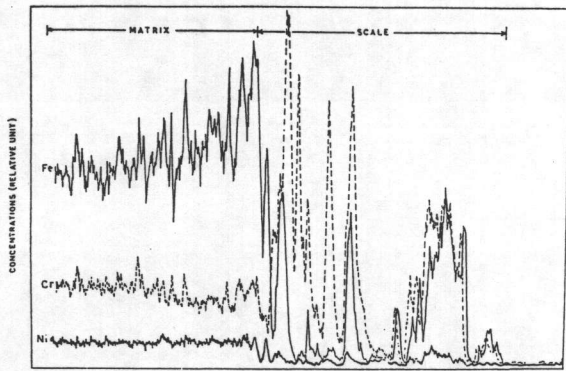17). The X-ray concentration profiles for the oxidized alloy show the presence of chromium-rich inner layers and iron-rich outer layers (Fig. 18).

The scanning electron micrograph of the oxidized $(Na_2SO_4 + CoSO_4)$ coated steel shows the presence of CoO and $CoSO_4$ in the outer scales (Fig. 19). The inner scales seem to contain

Fig. 18 Fe, Cr and Ni X-ray profiles across a scale formed on $Na_2SO_4 + NaVO_3$ coated steel oxidized at 1273 K.

Fig. 16 Fe, Cr and Ni X-ray profiles across a scale formed on $Na_2SO_4 + (NH_4)_2MoO_4$ coated steel oxidized at 1273 K.
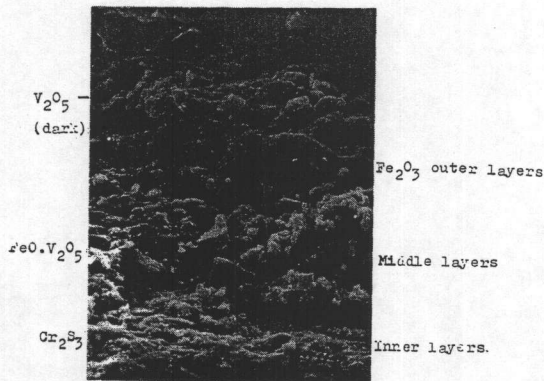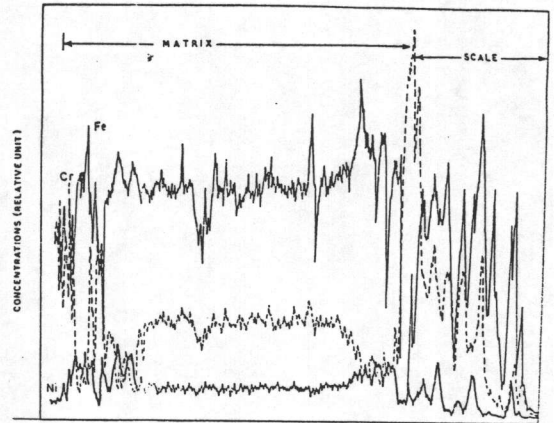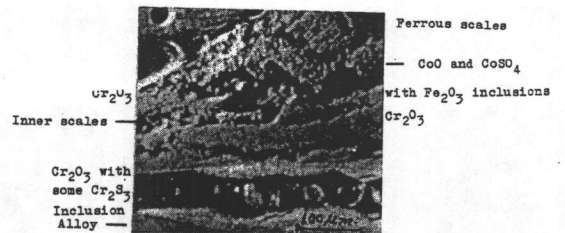

Fig. 19 SEM of $Na_2SO_4 + CoSO_4$ (9.8 + 14.0 g m^{-2}) coated steel oxidized at 1273 K.

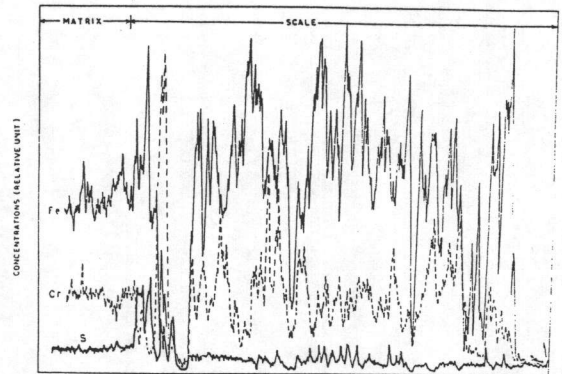Fig. 17 SEM of $Na_2SO_4 + NaVO_3$ (9.8 + 10 g m^{-2}) coated steel oxidized at 1273 K.

Fig. 20 Fe, Cr and S X-ray profiles across a scale formed on $Na_2SO_4 + CoSO_4$ coated steel oxidized at 1273 K.

Cr$_2$O$_3$ with Cr$_2$S$_3$ inclusions. The X-ray concentration profiles of the oxidized alloy provide similar information (Fig. 20).

IV.   Discussion

The oxidation behaviour of the 18Cr–8Ni steel coated with Na$_2$SO$_4$, transition metal salts or their mixtures falls into two general categories:

(i) The presence of NiSO$_4$ or Cr$_2$(SO$_4$)$_3$ in Na$_2$SO$_4$ enhances the oxidation rate of the Na$_2$SO$_4$ coated steel considerably at 923 K and 1123 K, whereas CoSO$_4$ shows this behaviour only at 923 K. At 1273 K, Na$_2$SO$_4$ coated steel has a higher oxidation rate than either Cr$_2$(SO$_4$)$_3$ or CoSO$_4$ coated steel.

Figure 21 represents a phase stability diagram obtained on superimposing stability diagrams for the Fe–S–O, Cr–S–O, Ni–S–O and Co–S–O systems at 1366 K. The diagram indicates sulphide and oxide phase stability regions and is useful in correlating the results of oxidation with those obtained from morphological studies.
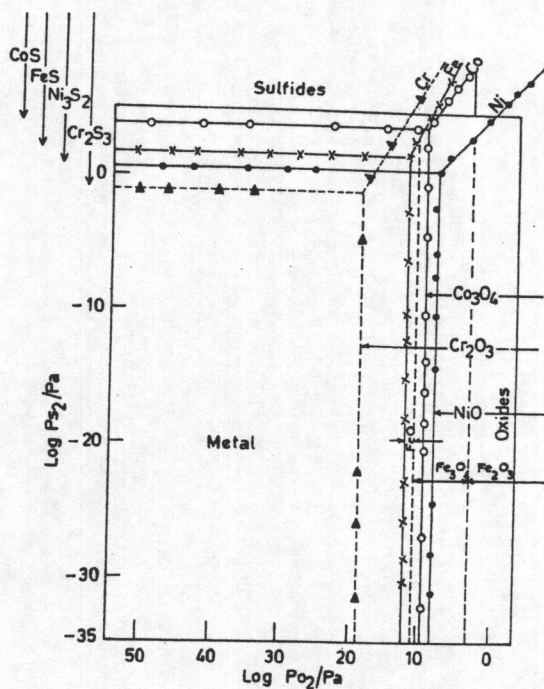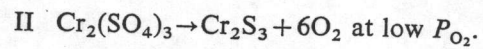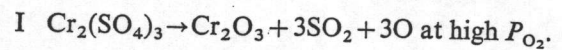

Fig. 21 Super-imposed phase stability diagrams for the metals Cr, Ni, Fe and Co with S and O at 1366 K.

(ii) (NH$_4$)$_2$MoO$_4$, Na$_2$WO$_4$ or NaVO$_3$ coated steels have invariably much higher oxidation rates than steel coated with a mixture of Na$_2$SO$_4$ or a mixture of Na$_2$SO$_4$ and transition metal salt in the temperature range of 923–1123 K. The oxidation behaviour of steel in presence of different salt coatings could be explained on the basis of the following considerations.

1.   Cr$_2$(SO$_4$)$_3$

Chromic sulphate can decompose as follows:

I   Cr$_2$(SO$_4$)$_3 \rightarrow$ Cr$_2$O$_3$ + 3SO$_2$ + 3O at high P_{O_2}.

II   Cr$_2$(SO$_4$)$_3 \rightarrow$ Cr$_2$S$_3$ + 6O$_2$ at low P_{O_2}.

At the oxide/salt interface, where the oxygen activity is low, reaction II may occur, whereas reaction I is favourable at the salt/air interface. It should also be emphasized that a Cr$_2$O$_3$ film will invariably be formed on the alloy during the coating process.

At lower temperatures (below 923 K), the mode of decomposition is governed by I. In that case, at the oxide/salt interface, Cr^{3+} and Fe^{2+} will slowly diffuse out to form Cr$_2$O$_3$ and FeO, respectively. The scale could consist of inner oxide layers of Cr$_2$O$_3$, middle layers of FeO and outer layers of Fe$_2$O$_3$. Due to the expulsion of SO$_2$, initially relatively low mass gains will be observed and the outer scales should be porous. A scale morphology of this type has indeed been observed.
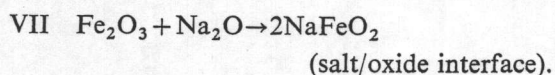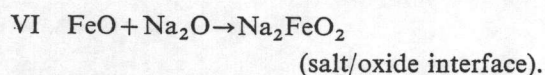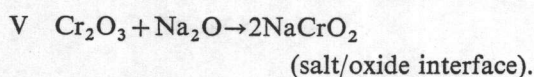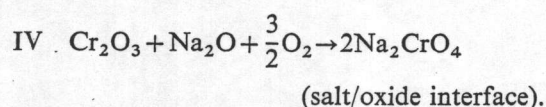
At higher temperature (1273 K) reaction II is favourable at the oxide/salt interface, whereas reaction I is favourable at the salt/air interface; conversion of Cr$_2$(SO$_4$)$_3$ into Cr$_2$S$_3$ will increase the activity of oxygen at the oxide/salt interface, resulting in the conversion of Cr$_2$S$_3$ into Cr$_2$O$_3$ and iron into FeO. Thus the scales should comprise inner scale containing small pockets of Cr$_2$S$_3$/FeCr$_2$S$_4$ followed by thicker layers of Cr$_2$O$_3$ and Fe$_2$O$_3$.

2.   Na$_2$SO$_4$ + Cr$_2$(SO$_4$)$_3$

At low temperature similar reactions as those observed in case of Cr$_2$(SO$_4$)$_3$ are expected. At high temperatures (above 923 K), Na$_2$SO$_4$ may decompose as

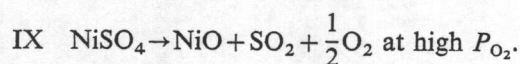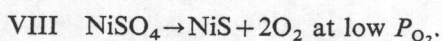III $SO_4^{--} \rightarrow O^{--} + S + \frac{3}{2}O_2$.
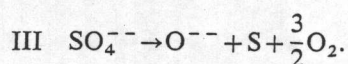
In such a situation at the oxide/salt interface, there would be sufficient activity of sulphur to form FeS and Cr_2S_3. The formation of sulphide will result in a decrease in the sulphur activity and consequently an increase in the oxygen activity. The increased oxygen activity at the oxide/salt interface results in the oxidation of some of the sulphides, and sulphur thus released is available for internal sulphidation. FeO and Cr_2O_3 formed as a result of oxidation of sulphides would flux with Na_2O (melt) to form Na_2FeO_2 and $Na_2CrO_4/NaCrO_2$.

IV $Cr_2O_3 + Na_2O + \frac{3}{2}O_2 \rightarrow 2Na_2CrO_4$

(salt/oxide interface).

V $Cr_2O_3 + Na_2O \rightarrow 2NaCrO_2$

(salt/oxide interface).

VI $FeO + Na_2O \rightarrow Na_2FeO_2$

(salt/oxide interface).

VII $Fe_2O_3 + Na_2O \rightarrow 2NaFeO_2$

(salt/oxide interface).

The reactions IV to VII are thermodynamically feasible. The reactions are likely to continue till all the Na_2O is consumed. At the salt/air interface a Na_2O is very low, and $NaCrO_2$ and Na_2CrO_4 would dissociate to precipitate Cr_2O_3. Similarly, FeO may be precipitated as a result of the dissociation of Na_2FeO_2.

3. NiSO$_4$

NiSO$_4$ (m.p. 1033 K and decomp. 1121 K) may decompose as follows:

VIII $NiSO_4 \rightarrow NiS + 2O_2$ at low P_{O_2}.

IX $NiSO_4 \rightarrow NiO + SO_2 + \frac{1}{2}O_2$ at high P_{O_2}.

At low temperatures (923 K) only reaction IX predominates. The outer layers of the scales should contain NiO enriched Fe_2O_3, and FeO and NiO forming the middle layers of the scale. Due to evolution of SO_2 the outer scales are porous, and relatively low mass gains are expected.

At temperatures above 1123 K, reaction VIII would be preferred at the oxide/salt interface besides reaction IX occurring at the salt/air interface. NiS may form a low melting eutectic with the nickel metal (m.p. 908 K), and the liquid eutectic would accumulate at the top of Cr_2O_3 or FeO layer and solidifies. The outer scales should have similar features to those found in coated steel oxidized at lower temperatures.

The steel coated with a mixture of NiSO$_4$ and Na$_2$SO$_4$ shows higher oxidation rates in the temperature range 923–1123 K due to the formation of a low melting eutectic (m.p. 940 K). At temperatures higher than 1123 K sulphidation reactions predominate.
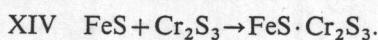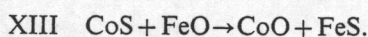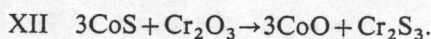
4. CoSO$_4$

CoSO$_4$ (m.p. 908 K with decomposition) decomposes in the following manner:

X $CoSO_4 \rightarrow CoO + SO_2 + \frac{1}{2}O_2$ at high P_{O_2}.

XI $CoSO_4 \rightarrow CoS + 2O_2$ at low P_{O_2}.
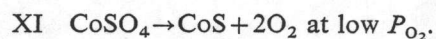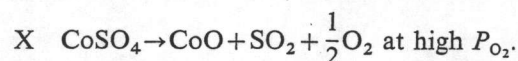
However, no CoS was detected in the scales of the oxidized alloy, therefore, there is a remote possibility of reaction XI occurring at the oxide/salt interface; this is also evident from Co–O–S equilibrium diagram (Fig. 21). In these circumstances, we expect a scale morphology, in which Cr_2O_3 forms the inner oxide scales, followed by a relatively thick scale comprising FeO and CoO, and Fe_2O_3 forms the outermost layer of the scale. A scale morphology of this type is evident from SEM studies.

In presence of Na$_2$SO$_4$ + CoSO$_4$ mixture, the low melting eutectic (m.p. 838 K) would penetrate through Cr_2O_3 and FeO films on the steel and may produce low temperature corrosion. At 923 K the steel coated with Na$_2$SO$_4$ + CoSO$_4$ mixture has higher oxidation rates than either Na$_2$SO$_4$ or CoSO$_4$ coated steel. At higher temperatures (1123–1273 K) reactions XI and III proceed at the oxide/salt interface forming CoS. In consequence, a region of low S-activity and high oxygen activity develops at the interface; subsequently CoS oxidizes to CoSO$_4$ or CoO according to the following reactions. Sulphur released during oxidation is mainly used up by chromium and iron to form sulphides, since their formations require much

lower sulphur potential (Fig. 21).

XII $\quad 3CoS + Cr_2O_3 \rightarrow 3CoO + Cr_2S_3$.

XIII $\quad CoS + FeO \rightarrow CoO + FeS$.

XIV $\quad FeS + Cr_2S_3 \rightarrow FeS \cdot Cr_2S_3$.

XV $\quad CoS + 2O_2 \rightarrow CoSO_4$.

Besides the reactions XII to XIV, there is some possibility of fluxing of iron oxides, as shown in VI and VII. The scale morphology would then comprise inner sulphide scales followed by the duplex oxide scales containing CoO and Cr$_2$O$_3$, and FeO and CoO with inclusions of CoSO$_4$.

5. Na$_2$WO$_4$

Na$_2$WO$_4$ (m.p. 971 K) decomposes according to the following reaction:

XVI $\quad Na_2WO_4 \rightarrow Na_2O + WO_3$.
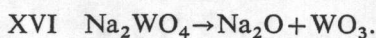
FeO which grows on Cr$_2$O$_3$ may react with Na$_2$O and WO$_3$ to form Na$_2$FeO$_2$ and FeWO$_4$, respectively.

XVII $\quad Na_2O + FeO \rightarrow Na_2FeO_2$.

XVIII $\quad WO_3 + FeO \rightleftarrows FeWO_4$.
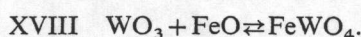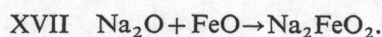
Dissolution of FeO in Na$_2$O will decrease the basicity of the melt, and WO$_3$ will dissolve through the process of acid fluxing precipitating as WO$_3$ at the air/salt interface (reaction XVIII in the reverse direction).

The scale morphology should then be consisting of Cr$_2$O$_3$ (inner), FeO–WO$_3$ with inclusions of Na$_2$FeO$_2$ and Na$_2$WO$_4$ (middle) and Fe$_2$O$_3$ with inclusions of WO$_3$ (outer).

At higher temperatures (1123 K and above) there is always a possibility of volatilization of WO$_3$, and this could result in catastrophic oxidation.

In presence of Na$_2$SO$_4$ and Na$_2$WO$_4$ the reactions XVI to XVIII are likely to occur along with some sulphidation reactions.

6. (NH$_4$)$_2$MoO$_4$

(NH$_4$)$_2$MoO$_4$ decomposes according to the following reaction:

XIX $\quad (NH_4)_2MoO_4 \rightarrow MoO_3 + 2NH_3 + H_2O$.
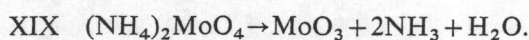
The MoO$_3$ formed according to reaction XIX will react with the FeO scale growing on the alloy (above Cr$_2$O$_3$ film) by cation diffusion forming FeO $\cdot$ MoO$_3$; there should be a rapid consumption of the steel, until the supply of MoO$_3$ is fully exhausted resulting in an enhanced oxidation rate for (NH$_4$)$_2$MoO$_4$ coated steel. This type of behaviour is expected in a wide range of temperature, however, higher concentrations of the salt and higher temperatures should facilitate volatilization of MoO$_3$, as is evident by the heavier mass losses observed during the oxidation (Fig. 3). The determinal effect of Mo in Ni- and Co-base alloys has been investigated in much detail[10].

At low temperatures (upto 1123 K) the steel coated with a mixture of Na$_2$SO$_4$ and (NH$_4$)$_2$MoO$_4$ shows almost the same behavious as that observed in case of molybdate coated steel. However, at high temperatures (above 1123 K) the following reactions are plausible:

i) Fluxing of FeO with Na$_2$O to form Na$_2$FeO$_2$.

ii) Reaction of MoO$_3$ with FeO to form FeO $\cdot$ MoO$_3$.

iii) Sulphidation of Fe and Cr to form FeS and Cr$_2$S$_3$.

iv) Precipitation of MoO$_3$ and FeO at the air/salt interface due to increased acidity of the melt or decrease in a_{Na_2O}.

The above reactions seem to be responsible for high oxidation rates of Na$_2$SO$_4$ + (NH$_4$)$_2$MoO$_4$ coated steel.

7. NaVO$_3$

Sodium metavanadate, NaVO$_3$ (m.p. 903 K), decomposes according to the following reaction:
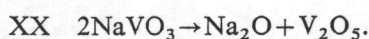
XX $\quad 2NaVO_3 \rightarrow Na_2O + V_2O_5$.

In steel coated with NaVO$_3$, Na$_2$O formed during the decomposition reacts with FeO or Fe$_2$O$_3$ to form Na$_2$FeO$_2$ or Na$_2$Fe$_2$O$_4$ (reactions VI and VII). V$_2$O$_5$ may also react with FeO to form FeO $\cdot$ V$_2$O$_5$ (reaction XXI) at relatively low temperatures.

XXI $\quad FeO + V_2O_5 \rightarrow FeO \cdot V_2O_5$.
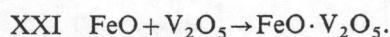
However, at higher temperatures (above 923 K), volatilization of V$_2$O$_5$ (b.p. 948 K) is preferable to reaction XXI. This may result in the catastrophic oxidation of the steel.

Since the addition of Na_2SO_4 to $NaVO_3$ is likely to suppress the dissociation of $NaVO_3$ (reaction XX) or the formation of V_2O_5. In consequence, there will be lesser amount of V_2O_5 available for volatilization, and therefore, the presence of Na_2SO_4 in $NaVO_3$ lowers the oxidation rate of coated steel.

V. Conclusions

(1) The higher oxidation rates for $Na_2SO_4 + CoSO_4$, and $Na_2SO_4 + NiSO_4$ coated steels at 923 K in comparison with the corresponding Na_2SO_4 or transition metal sulphate coated steel have been attributed to the formation of low temperature eutectics.

(2) $Cr_2(SO_4)_3$ coated steel has the lowest oxidation rate in the temperature range between 923 K and 1273 K.

(3) The presence of Na_2WO_4, $(NH_4)_2 MoO_4$ or $NaVO_3$ is always detrimental to the oxidation resistance of steel especially in the temperature range of 1123–1273 K. The decomposition of these salts into volatile oxides seems to be the main reason of catastrophic oxidation. In fact the transition metal salt coated steel has a much higher oxidation rate than Na_2SO_4 coated steel.

(4) A direct oxidation mechanism is sufficient to explain the corrosion of tranistion metal salt coated steel. However, the steel coated with a mixture of Na_2SO_4 and transition metal salt requires sulphidation cum fluxing mechanism to explain hot corrosion.

REFERENCES

(1) W. T. Reid: *External Corrosion and Deposits— Boilers and Gas turbines*, Elsvier, New York, (1971).

(2) R. W. Borio, A. L. Plumley and W. R. Sylvester: *Proc. of the Int. Conf. on Ash Deposits and Corrosion from Impurities in Combustion Gases*, Henniker, New Hampshire (1977).

(3) Hendry and D. J. Lees: Corros. Sci., **20** (1980), 383.

(4) K. A. Bol'shakov, P. I. Federov and N. I. Il'ina: Russ. J. Inorg. Chem. (Eng. Trans.), (1963), 1351.

(5) A. Rahmel and W. Jaeger: Z. anorg. Chem., **303** (1960), 90.

(6) C. Cain and W. Nelson: Am. Soc. Mech. Engnrs Paper, 60-WA-180 (1961).

(7) K. L. Luthra: presented at the NACE Int. Conf. on High Temp. Corrosion. San Diego, March 2–6, 1981.

(8) R. L. Jones: ibid.

(9) R. L. Jones and S. T. Gadomski: J. Electrochem. Soc., **129** (1982), 1613.

(10) J. Stringer: Ann. Rev. Mater. Sci., **7** (1977), 477.

(11) P. C. Hemmings and R. A. Perkins: Lockheed Palo Alto Research Laboratories, report to EPRI on Project No. RP 716–1, March 1977.